444. *Triterpenoids. The Crystal Structure of Lanostenyl Iodoacetate.*

By J. FRIDRICHSONS and A. McL. MATHIESON.

The crystal structure of lanostenyl iodoacetate has been determined by *X*-ray analysis. Parameters of all atoms (except hydrogen) have been fixed, providing without ambiguity the structural formula and a detailed stereochemical description of the molecule. Lanostenol has a tetradecahydro*cyclo*pentenophenanthrene ring system with an inert double bond at $C_{(9)}$–$C_{(10)}$ (triterpenoid notation), the rings A and B and C and D being *trans*-fused. The $C_{(2)}$-hydroxyl group and the $C_{(5)}$- and $C_{(13)}$-methyl groups are β-oriented whereas that at $C_{(14)}$ is α-oriented. The *gem*-dimethyl group is attached to $C_{(1)}$ and the side-chain to $C_{(17)}$.

Distortions arising from the intramolecular packing of methyl groups and from the fusion of the five- to the six-membered rings have been observed. The structure of lanostenol shows remarkable similarity to that of cholesterol.

WOOL-WAX (for references see the review by Velluz and Lederer, *Bull. Soc. Chim. biol.*, 1945, **27**, 211) contains at least four triterpenoid components: lanostenol (dihydrolanosterol) $C_{30}H_{52}O$ (I), lanostadienol (lanosterol) $C_{30}H_{50}O$ (II), agnostadienol (dihydroagnosterol) or (γ-lanosterol) $C_{30}H_{50}O$ (III), and agnostatrienol (agnosterol) $C_{30}H_{48}O$ (IV). These four compounds are probably based on the same carbon skeleton involving a tetracyclic ring system. Since the solution of the structure of one member would provide a key to those of the other three, lanostenyl iodoacetate was selected as a suitable " heavy-atom " derivative for single-crystal *X*-ray analysis, this technique having been applied with success to steroid molecules of similar complexity: cholesterol (Carlisle and Crowfoot, *Proc. Roy. Soc.*, 1945, *A*, **184**, 64) and calciferol (Crowfoot and Dunitz, *Nature*, 1948, **162**, 608). Structure determination by this method can provide an unequivocal picture of the structure and the stereochemical details of the molecule.

During the present work, Cavalla, McGhie, and Pradhan (*J.*, 1951, 3142), Barton, Fawcett, and Thomas (*J.*, 1951, 3147), Voser, Mijovic, Jeger, and Ruzicka (*Helv. Chim. Acta*, 1951, **34**, 1585), Voser, Guenthard, Jeger, and Ruzicka (*ibid.*, 1952, **35**, 66) and Barnes, Barton, Fawcett, Knight, McGhie, Pradhan, and Thomas (*Chem. and Ind.*, 1951, 1067) have brought forward chemical and spectrophotometric evidence which established an almost complete structural formula for the lanostenol molecule. However, the point of linkage of the side chain to the ring system has remained in doubt. Barnes, Barton, Fawcett, and Thomas (*J.*, 1952, 2339) favoured $C_{(15)}$ or $C_{(16)}$ on the assumption that the " isoprene rule " holds. In a later publication (*Chem. and Ind.*, 1952, 426), Barnes, Barton, Cole, Fawcett, and Thomas adduced infra-red and chemical evidence which reduced the possibilities to $C_{(15)}$ and $C_{(17)}$, the former again being favoured. Voser, White, Heusser, Jeger, and Ruzicka (*Helv. Chim. Acta*, 1952, **35**, 830) and Mijovic, Voser, Heusser, and Jeger (*ibid.*, p. 964) located the chain at $C_{(17)}$, but have not so far provided experimental evidence for this decision.

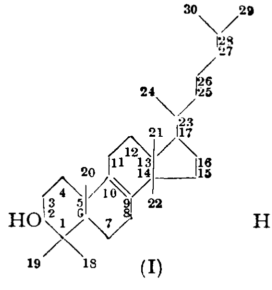

(I)

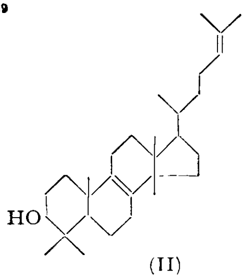

(II)

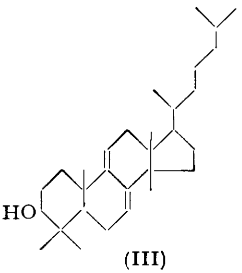

(III)

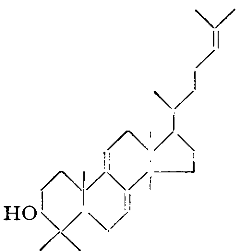

(IV)

No chemical evidence on the stereochemistry of lanostenol has been given previously, although Barton, Fawcett, and Thomas (*loc. cit.*), on the basis of a ring structure involving four six-membered rings, have offered some comments (*loc. cit.* Fig. V)—omitting any consideration of the influence of the double bond.

Since a brief report of our investigation has been made (*Nature*, 1952, 170, 221), this paper deals with the detailed structural analysis and discusses the stereochemistry of lanostenol in relation to the other wool-wax triterpenoids, and steroids of similar structure.

EXPERIMENTAL

Crystals of lanostenyl acetate, chloroacetate, and iodoacetate were prepared by Mr. R. Curtis (*J.*, 1950, 1017). Exploratory rotation and moving-films measurements indicated that their unit-cell dimensions differed too greatly for these crystals to be treated as isomorphous. Lanostenyl iodoacetate, $C_{32}H_{53}O_2I$, was therefore selected as the most suitable compound for structure analysis by the " heavy-atom " technique.

Slow cooling of a hot chloroform–methanol solution gave the iodoacetate as thin transparent lath-like crystals, elongated along the *a* axis. The crystals used in recording rotation and Weissenberg photographs were approximately 0·6 × 0·4 × 0·1 mm. The unit cell is orthorhombic with dimensions $a = 7{\cdot}6$, $b = 10{\cdot}9$, and $c = 38{\cdot}6$ Å. Reflections $h00$, $0k0$, and $00l$ are absent in odd orders, indicating the space group $P2_12_12_1$. The density, calculated for four molecules, is 1·24 g./cm.^{3}, the measured value being 1·25 g./cm.^{3}.

An attempt was made to obtain thicker crystals by slow crystallization from various solvents. Crystals from ethyl acetate had nearly perfect square cross-section but on examination were found to be a dimorph with the *a* axis doubled (*i.e.*, eight molecules per unit cell). Only this second form could be obtained on subsequent recrystallizations in this laboratory. Accordingly, the structure analysis had to be carried out on the batch of crystals of the simpler dimorph derived from the earlier crystallizations.

Intensity data for the $0kl$ and $h0l$ reflections were recorded on multiple-film packs, exposed in a Weissenberg goniometer. Two packs, related by timed exposures, were utilised and the intensities were estimated visually against a set of standards, a range of intensities of 1 to 1500 being covered. No corrections for absorption were applied to the intensity data. The structure amplitudes of the two zones were placed on the same scale by correlation of the common $00l$ reflections and were later set on an absolute basis by comparison with the values calculated on the basis of the f curves for carbon, oxygen, and iodine, given in the " International Tables " (Bornträger, Berlin, 1936). The temperature factor to be applied to the calculated structure amplitudes, $B = 5{\cdot}75 \times 10^{-16}$ cm.^{2}, was obtained by plotting log $(\Sigma|F_c|/|F_0|)$ against $\sin^2\theta$ over small equal ranges of $\sin^2\theta$.

Fourier summations were carried out by means of three-figure Beevers–Lipson strips with 12° intervals along the *a*- and *b*-axes and 3° intervals along the *c* axis. In the final synthesis for each projection, a better approximation to the correct electron-density distribution was attained by adding into the Fourier synthesis the calculated values of structure amplitudes of reflections whose intensity lay below the limit of observation in the particular experiment.

Structure Analysis.—The parameters of the iodine atoms were derived from Patterson projections, $P(y, z)$ and $P(x, z)$. The contributions of the iodine atoms to the $0kl$ and $h0l$ structure amplitudes were calculated and, since the projections down the *a*- and *b*-axes are centrosymmetric, it could be assumed that the " heavy-atom " contribution would determine correctly the signs of the majority of observed structure amplitudes, except those with small or vanishing iodine contribution; for instance, all $05l$ terms with l odd had to be omitted until the final refinement synthesis.

The first Fourier syntheses for the *a*- and *b*-axis projections were computed with 113 and 63 terms, respectively. The electron-density distribution along the *a*-axis showed ridges of high electron-density, approximately 20 Å long, clearly separated and lying at approximately 30° to the *c*-axis. It was considered that the individual ridges corresponded to an elongated, lath-shaped molecule, with the " plane " of the molecular ring system lying approximately normal to (100) and hence this projection represented an edge-on view of the molecule. There was no overlapping of molecules, but, owing to the small number of Fourier terms, most atoms were not resolved and false peaks near the iodine atom made it impossible to locate the acetate group. The *b*-axis projection, which was thus expected to show the molecule viewed side-on, gave still less resolution and indicated moreover a probable partial overlap of the molecules.

Attention was therefore focused on the *a*-axis projection as more likely to yield to interpretation. The second Fourier synthesis was computed, utilising additional terms from a

TABLE 1. *Comparison of the observed and calculated structure amplitudes for lanostenyl iodoacetate.*

hkl	$F_{obs.}$	$F_{calc.}$	*hkl*	$F_{obs.}$	$F_{calc.}$	*hkl*	$F_{obs.}$	$F_{calc.}$	*hkl*	$F_{obs.}$	$F_{calc.}$
000		+1256	026	19	+13	0,3,38	<20	−1	0,5,30	36	+40
002	80	−109	027	132	+151	0,3,39	21	+21	0,5,31	<20	+3
004	110	+151	028	23	+3	0,3,40	<20	+1	0,5,32	21	−30
006	144	−175	029	158	−142	0,3,41	20	−20	0,5,33	<20	0
008	151	+167	0,2,10	73	+80				0,5,34	<20	+13
0,0,10	140	−168	0,2,11	94	+98	040	125	−131	0,5,35	<20	0
0,0,12	220	+209	0,2,12	23	−22	041	105	+110	0,5,36	20	−20
0,0,14	157	−144	0,2,13	49	−76	042	104	+123			
0,0,16	61	+74	0,2,14	<15	+33	043	75	−78	060	51	+59
0,0,18	72	−64	0,2,15	26	+54	044	93	−98	061	46	+40
0,0,20	90	+69	0,2,16	30	−10	045	43	+55	062	68	−82
0,0,22	33	−21	0,2,17	43	−63	046	108	+85	063	80	−54
0,0,24	90	+72	0,2,18	<15	+13	047	30	−31	064	60	+77
0,0,26	<20	+5	0,2,19	73	+74	048	29	−30	065	24	+45
0,0,28	35	+20	0,2,20	<15	−18	049	174	+164	066	43	−58
0,0,30	<20	−3	0,2,21	16	−40	0,4,10	36	+42	067	93	−95
0,0,32	24	+9	0,2,22	17	+2	0,4,11	21	−41	068	61	+75
0,0,34	<20	+4	0,2,23	17	+26	0,4,12	153	−134	069	34	+54
0,0,36	36	+8	0,2,24	18	−24	0,4,13	30	+40	0,6,10	53	−54
0,0,38	<20	+8	0,2,25	<18	−21	0,4,14	68	+63	0,6,11	42	−38
0,0,40	23	−14	0,2,26	25	−6	0,4,15	77	−75	0,6,12	26	+48
			0,2,27	<20	+8	0,4,16	72	−65	0,6,13	<16	−2
011	76	+71	0,2,28	<20	−9	0,4,17	<18	+21	0,6,14	18	−40
012	17	+13	0,2,29	<20	−14	0,4,18	55	+44	0,6,15	32	−25
013	80	−74	0,2,30	28	−3	0,4,19	<18	−26	0,6,16	17	+42
014	102	−89	0,2,31	<20	−1	0,4,20	19	−24	0,6,17	44	+47
015	24	−26	0,2,32	<20	−2	0,4,21	<18	+23	0,6,18	22	−27
016	91	−80	0,2,33	<20	−5	0,4,22	19	+20	0,6,19	<18	−11
017	59	−56	0,2,34	<20	+9	0,4,23	29	−24	0,6,20	<18	+27
018	60	+63	0,2,35	38	−14	0,4,24	34	−29	0,6,21	30	+21
019	96	+86	0,2,36	<20	+2	0,4,25	35	+2	0,6,22	<20	−17
0,1,10	51	−54	0,2,37	<20	+9	0,4,26	18	+18	0,6,23	34	−25
0,1,11	<15	−10	0,2,38	20	−14	0,4,27	<18	+4	0,6,24	<20	+25
0,1,12	86	+87				0,4,28	20	−13	0,6,25	20	−6
0,1,13	42	+47	031	9	+9	0,4,29	<20	+8	0,6,26	24	−4
0,1,14	91	−85	032	23	+38	0,4,30	<20	−4	0,6,27	<20	−12
0,1,15	15	−23	033	91	+81	0,4,31	28	+12	0,6,28	<20	+14
0,1,16	49	+61	034	54	+48	0,4,32	<20	−4	0,6,29	32	+20
0,1,17	15	+27	035	66	−64	0,4,33	20	−8	0,6,30	<20	−14
0,1,18	95	−83	036	34	−36	0,4,34	<20	+6	0,6,31	<20	+2
0,1,19	91	−78	937	140	+93	0,4,35	<20	+2	0,6,32	<20	+4
0,1,20	73	+78	038	40	+43				0,6,33	20	−11
0,1,21	49	+52	039	36	−42	051	45	−26			
0,1,22	55	−46	0,3,10	42	+33	052	<16	+4	071	17	+8
0,1,23	21	−26	0,3,11	63	+65	053	<16	0	072	<16	+8
0,1,24	68	+65	0,3,12	50	+38	054	16	−21	073	34	−30
0,1,25	26	+35	0,3,13	63	−66	055	20	+5	074	16	+8
0,1,26	63	−53	0,3,14	74	−73	056	24	−32	075	<16	+24
0,1,27	28	−32	0,3,15	100	+94	057	56	−28	076	<16	+5
0,1,28	32	+43	0,3,16	36	+1	058	77	−54	077	17	−30
0,1,29	28	+27	0,3,17	72	−70	059	<18	−10	078	21	+21
0,1,30	37	−44	0,3,18	<18	−26	0,5,10	43	+44	079	<18	+14
0,1,31	34	−33	0,3,19	60	+70	0,5,11	76	−48	0,7,10	<18	+11
0,1,32	30	+40	0,3,20	<18	+7	0,5,12	71	−63	0,7,11	<18	−4
0,1,33	<20	+15	0,3,21	45	−56	0,5,13	24	−27	0,7,12	21	+9
0,1,34	<20	−14	0,3,22	<18	−7	0,5,14	18	+24	0,7,13	56	+59
0,1,35	20	−15	0,3,23	76	+78	0,5,15	42	−30	0,7,14	21	−16
0,1,36	<20	+24	0,3,24	21	+21	0,5,16	21	−29	0,7,15	<18	−35
0,1,37	28	+26	0,3,25	41	−51	0,5,17	<18	−1	0,7,16	18	+8
0,1,38	<20	−4	0,3,26	30	−30	0,5,18	71	+70	0,7,17	32	+44
0,1,39	21	−20	0,3,27	67	+60	0,5,19	<18	−5	0,7,18	<20	−10
0,1,40	<20	+8	0,3,28	<20	+8	0,5,20	22	−29	0,7,19	21	−36
0,1,41	<20	+10	0,3,29	21	−31	0,5,21	18	−4	0,7,20	<20	+13
0,1,42	20	−16	0,3,30	25	−22	0,5,22	37	+47	0,7,21	33	+40
			0,3,31	34	+40	0,5,23	<18	−4	0,7,22	21	−21
020	62	−71	0,3,32	20	+15	0,5,24	30	−43	0,7,23	24	−36
021	47	−53	0,3,33	30	−34	0,5,25	28	−27	0,7,24	<20	+11
022	23	+4	0,3,34	23	−17	0,5,26	19	+29	0,7,25	21	+34
023	49	+50	0,3,35	30	+34	0,5,27	29	−24	0,7,26	<20	−10
024	256	−236	0,3,36	<20	+10	0,5,28	30	−35	0,7,27	20	−37
025	292	−299	0,3,37	21	−24	0,5,29	<20	+3	0,7,28	<20	+10

TABLE 1. (*Continued.*)

hkl	$F_{obs.}$	$F_{calc.}$	*hkl*	$F_{obs.}$	$F_{calc.}$	*hkl*	$F_{obs.}$	$F_{calc.}$	*hkl*	$F_{obs.}$	$F_{calc.}$
0,7,29	20	+26	101	69	+73	2,0,24	<18	+20	4,0,11	41	−47
0,7,30	<20	+7	102	<10	−4	2,0,25	29	−33	4,0,12	<18	−3
0,7,31	20	−18	103	201	+173	2,0,26	<20	+20	4,0,13	23	−35
			104	44	+25	2,0,27	<20	−29	4,0,14	33	+24
080	27	+19	105	184	+153	2,0,28	<20	0	4,0,15	24	−40
081	<18	−40	106	94	−52	2,0,29	33	−37	4,0,16	<18	−4
082	25	−22	107	129	+117				4,0,17	42	−49
083	66	+71	108	41	−44	301	88	+79	4,0,18	<20	−1
084	<18	+11	109	153	+158	302	<15	−7	4,0,19	32	−51
085	28	−48	1,0,10	54	−46	303	61	+70	4,0,20	<20	−10
086	<18	−4	1,0,11	70	+102	304	59	−52	4,0,21	25	−31
087	32	+50	1,0,12	15	−20	305	92	+70	4,0,22	<20	−7
088	<18	−3	1,0,13	62	+89	306	<15	−18	4,0,23	36	−53
089	<18	−34	1,0,14	35	−46	307	49	+41	4,0,24	<20	−4
0,8,10	19	−23	1,0,15	102	+113	308	56	+26	4,0,25	<20	−34
0,8,11	<20	+40	1,0,16	18	−37	309	28	+35	4,0,26	<20	+5
0,8,21	<20	+18	1,0,17	18	+37	3,0,10	24	−23	4,0,27	27	−35
0,8,13	20	−42	1,0,18	35	−25	3,0,11	119	+89	4,0,28	<20	−5
0,8,14	<20	−23	1,0,19	49	+58	3,0,12	93	−83	4,0,29	<20	−10
0,8,15	21	+31	1,0,20	54	−54	3,0,13	<16	+18	4,0,30	<20	+2
0,8,16	20	+15	1,0,21	44	+55	3,0,14	80	−76	4,0,31	27	−33
0,8,17	<20	−24	1,0,22	31	−29	3,0,15	33	+27			
0,8,18	27	−15	1,0,23	29	+29	3,0,16	24	−48	501	<18	−22
0,8,19	<20	+24	1,0,24	41	−43	3,0,17	26	+23	502	<18	+2
0,8,20	<20	−4	1,0,25	<20	+18	3,0,18	51	−58	503	<18	−22
0,8,21	<20	−10	1,0,26	29	−26	3,0,19	<18	+20	504	28	−23
0,8,22	20	−12				3,0,20	24	−46	505	34	−39
			200	48	+80	3,0,21	<18	+20	506	<18	−10
091	29	+11	201	<10	+23	3,0,22	21	−29	507	<18	−28
092	<20	0	202	87	+82	3,0,23	<18	+10	508	<18	−15
093	30	+30	203	11	+8	3,0,24	41	−50	509	32	−24
094	<20	−3	204	150	+118	3,0,25	25	+20	5,0,10	33	−30
095	20	+7	205	61	−53	3,0,26	41	−49	5,0,11	<20	−23
096	<20	−8	206	68	+84	3,0,27	<20	+1	5,0,12	<20	−32
097	<20	−4	207	78	−60	3,0,28	43	−50	5,0,13	<20	−20
098	<20	+15	208	123	+108	3,0,29	<20	+11	5,0,14	<20	−22
099	20	−15	209	72	−59	3,0,30	40	−44	5,0,15	25	−17
0,9,10	20	−26	2,0,10	50	+55	3,0,31	<20	−17.			
0,9,11	20	+13	2,0,11	21	−42	3,0,32	23	−22	600	<20	−23
0,9,12	<20	+27	2,0,12	56	+77				601	35	−22
0,9,13	20	−13	2,0,13	18	+6	400	<15	−13	602	55	−57
			2,0,14	38	+52	401	54	+25	603	39	−22
0,10,0	<20	−36	2,0,15	64	−66	402	17	−4	604	<20	−19
0,10,2	24	+45	2,0,16	<16	+25	403	53	−35			
0,10,4	<20	−32	2,0,17	<16	−30	404	<15	−19	701	<20	−22
0,10,6	32	+46	2,0,18	17	+42	405	17	−10	702	<20	+7
0,10,8	20	−36	2,0,19	37	−59	406	35	−17	703	<20	−24
0,10,10	23	+32	2,0,20	31	+39	407	65	−59	704	<20	−4
			3,0,21	35	−44	408	<16	−5	705	24	−33
0,11,1	20	−21	2,0,22	19	+28	409	38	−37			
0,11,3	20	+6	2,0,23	<18	−26	4,0,10	34	−30			

TABLE 2. *Atomic parameters*

Atom	*x*	*y*	*z*	Atom	*x*	*y*	*z*	Atom	*x*	*y*	*z*
I	0·064	−0·095	0·258	$C_{(10)}$	0·500	0·289	0·086	$C_{(22)}$	0·658	0·564	0·078
$O_{(1)}$	0·372	0·184	0·261	$C_{(11)}$	0·317	0·356	0·076	$C_{(23)}$	0·511	0·564	−0·042
$O_{(2)}$	0·400	0·061	0·217	$C_{(12)}$	0·333	0·461	0·044	$C_{(24)}$	0·320	0·600	−0·036
$C_{(1)}$	0·589	0·103	0·165	$C_{(13)}$	0·506	0·466	0·025	$C_{(25)}$	0·634	0·667	−0·060
$C_{(2)}$	0·432	0·131	0·189	$C_{(14)}$	0·667	0·483	0·050	$C_{(26)}$	0·556	0·678	−0·097
$C_{(3)}$	0·267	0·131	0·167	$C_{(15)}$	0·855	0·489	0·035	$C_{(27)}$	0·661	0·758	−0·117
$C_{(4)}$	0·286	0·222	0·138	$C_{(16)}$	0·816	0·567	−0·001	$C_{(28)}$	0·645	0·767	−0·153
$C_{(5)}$	0·464	0·214	0·117	$C_{(17)}$	0·600	0·555	−0·004	$C_{(29)}$	0·767	0·865	−0·175
$C_{(6)}$	0·603	0·189	0·139	$C_{(18)}$	0·600	−0·033	0·158	$C_{(30)}$	0·467	0·842	−0·164
$C_{(7)}$	0·765	0·186	0·114	$C_{(19)}$	0·753	0·111	0·189	$C_{(31)}$	0·300	−0·017	0·267
$C_{(8)}$	0·789	0·308	0·094	$C_{(20)}$	0·442	0·117	0·092	$C_{(32)}$	0·342	0·095	0·244
$C_{(9)}$	0·634	0·372	0·079	$C_{(21)}$	0·542	0·350	0·003				

TABLE 3. *Intramolecular bond lengths and intermolecular approach distances.*

(a) *Intramolecular bond lengths.*

	Å		Å		Å		Å
I–$C_{(31)}$	2·02	$C_{(4)}$–$C_{(5)}$	1·57	$C_{(11)}$–$C_{(12)}$	1·69	$C_{(17)}$–$C_{(23)}$	1·59
$C_{(31)}$–$C_{(32)}$	1·52	$C_{(5)}$–$C_{(6)}$	1·39	$C_{(12)}$–$C_{(13)}$	1·51	$C_{(23)}$–$C_{(24)}$	1·52
$C_{(32)}$–$O_{(1)}$	1·19	$C_{(5)}$–$C_{(20)}$	1·44	$C_{(13)}$–$C_{(14)}$	1·56	$C_{(23)}$–$C_{(25)}$	1·62
$C_{(32)}$–$O_{(2)}$	1·24	$C_{(6)}$–$C_{(7)}$	1·54	$C_{(14)}$–$C_{(9)}$	1·67	$C_{(25)}$–$C_{(26)}$	1·56
$C_{(2)}$–$O_{(2)}$	1·33	$C_{(6)}$–$C_{(1)}$	1·39	$C_{(13)}$–$C_{(21)}$	1·55	$C_{(26)}$–$C_{(27)}$	1·40
$C_{(1)}$–$C_{(2)}$	1·53	$C_{(7)}$–$C_{(8)}$	1·54	$C_{(14)}$–$C_{(22)}$	1·39	$C_{(27)}$–$C_{(28)}$	1·41
$C_{(1)}$–$C_{(18)}$	1·51	$C_{(8)}$–$C_{(9)}$	1·50	$C_{(14)}$–$C_{(15)}$	1·56	$C_{(28)}$–$C_{(29)}$	1·64
$C_{(1)}$–$C_{(19)}$	1·55	$C_{(9)}$–$C_{(10)}$	1·38	$C_{(15)}$–$C_{(16)}$	1·66	$C_{(28)}$–$C_{(30)}$	1·64
$C_{(2)}$–$C_{(3)}$	1·52	$C_{(10)}$–$C_{(5)}$	1·47	$C_{(16)}$–$C_{(17)}$	1·66		
$C_{(3)}$–$C_{(4)}$	1·52	$C_{(10)}$–$C_{(11)}$	1·61	$C_{(17)}$–$C_{(13)}$	1·64		

Mean C–C: 1·54 ± 0·09 Å.

(b) *Intermolecular approach distances.*

	Å		Å		Å		Å
I–$O_{(1)}$	5·7	$C_{(20)}$–$C_{(23)}$	5·0	$C_{(32)}$–$C_{(29)}$	3·9	$C_{(18)}$–$C_{(27)}$	5·1
$O_{(1)}$–$C_{(30)}$	3·9	$C_{(31)}$–$C_{(30)}$	4·0	$C_{(22)}$–$C_{(27)}$	4·5	$C_{(18)}$–$C_{(26)}$	4·4
$C_{(28)}$–$C_{(18)}$	4·8	$C_{(20)}$–$C_{(24)}$	4·2	$C_{(22)}$–$C_{(26)}$	5·4	$C_{(31)}$–$C_{(28)}$	5·0
$C_{(21)}$–$C_{(21)}$	4·4	$C_{(32)}$–$C_{(30)}$	4·4	$C_{(22)}$–$C_{(25)}$	5·0		

120-hour moving-film exposure, the signs being fixed by the iodine atom contribution. This distribution showed improved resolution but still did not permit location of the acetate group for the following reasons: (1) the number of peaks adjacent to the iodine atom was greater than necessary to account for the acetate group; (2) the inability to obtain accurate cell dimensions, owing to the large temperature factor, made it necessary to keep in mind the possibility that a molecule of the solvent might be included in the structure adjacent to the iodine atom; (3) both ends of the ridge were adjacent to iodine atoms and there was no distinctive indication at this stage about which end of the ridge (molecule) the acetate group was related to.

FIG. 1. *Partial difference synthesis, $\rho(z)$-$\rho_1(z)$.*

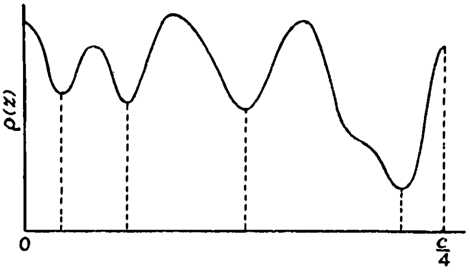

FIG. 2. *The final electron-density distribution projected on (100).*

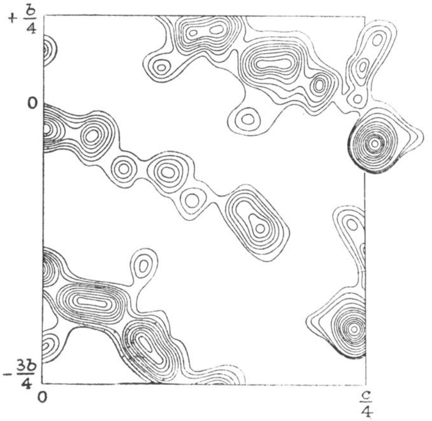

Contours for the iodine atom are drawn at intervals of 5 eA^{-2} *and for other atoms at* 1 eA^{-2}. *The lowest contour value shown is* 2 eA^{-2}.

It was therefore clear that progress in the analysis would be prevented until the acetate group was located. This problem was resolved by computing the uni-dimensional Fourier synthesis $\rho(z)$ (Fig. 1, with the iodine atom removed) and evaluating the number of atoms at different levels. This revealed that there could be only three atoms (of the asymmetric unit) near the level $z = 0{\cdot}25$ and that there was none or at most only one atom in the region $z = 0{\cdot}225$. Hence, with the known bond-lengths and angles of the iodoacetate group and account being taken of the electron-density distribution near the iodine atom in the *b*-axis projection, the number of sterically possible positions of the acetate group was reduced. When the acetate group was located in space, this determined which end of the ridge corresponded to the ring system since it was known that the acetate group was directly linked to ring A. Furthermore, it was then apparent that the other end of the ridge must correspond to the side chain. Successive trial models for the molecule were fitted to the projection, and structure amplitudes calculated. Since the molecular models could not deviate far from the region indicated by the ridge but merely differ in minor details, the calculation of structure amplitudes (at this stage, the reliability factor, $R = \Sigma|F_0 - F_c|/\Sigma|F_0| = 0.38$) permitted some additional signs to be fixed. By

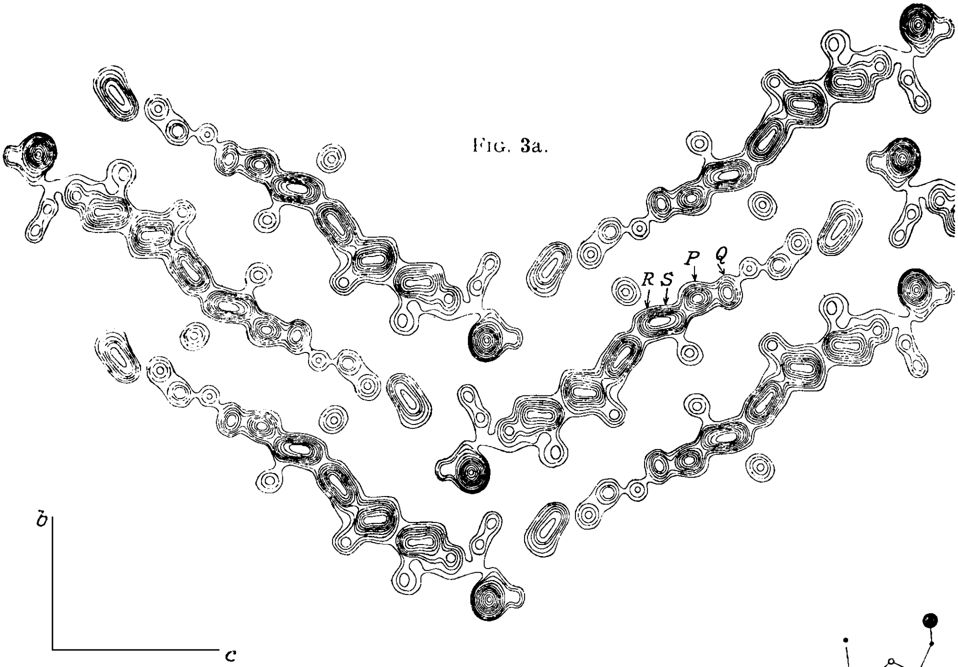
FIG. 3a.

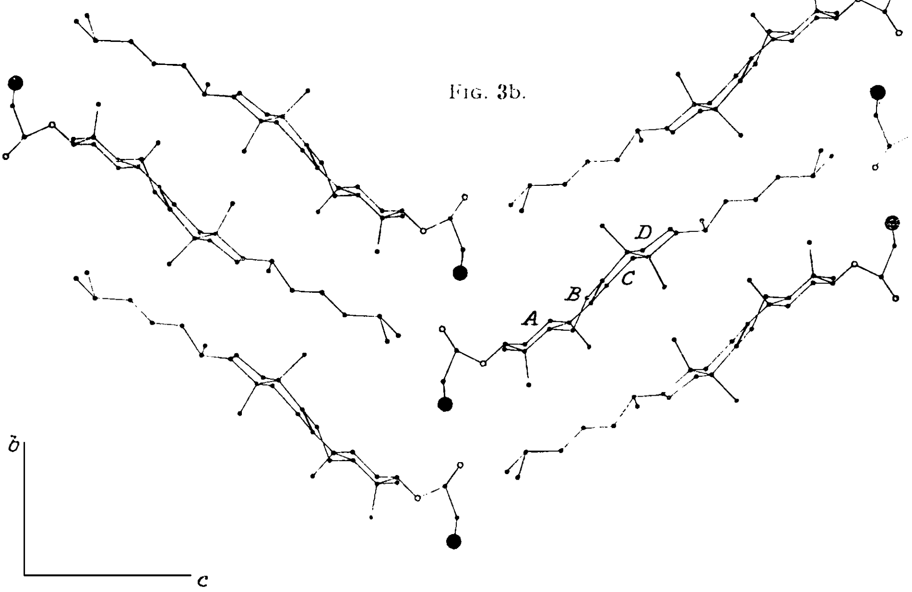
FIG. 3b.

FIG. 3a. *The electron-density distribution, ρ(y, z), extended over several unit cells to illustrate the molecular packing in the crystal. The penultimate electron-density distribution was used to compose this figure, and thus the contour distribution differs slightly from that of Fig. 2.*

FIG. 3b. *The corresponding diagram of the crystal structure.*

repeated Fourier syntheses, the reliability factor for this projection was reduced to 0·25 and the main outlines of the structure, *i.e.*, location of the ring system, disposition of the side methyl groups, and the configuration of the side chain became more evident.

Since the y and z co-ordinates of all atoms were thus fixed with reasonable accuracy, it was possible to return to the interpretation of the b-axis projection in order to determine the x co-ordinates and to confirm some points of the structure which could not be decisively derived from the a-axis projection alone since this presented only an edge-on view of the molecule. By utilising nearly all the $h0l$ structure amplitude terms available, Fourier synthesis yielded the electron-density distribution $\rho(x, z)$ on which all atomic positions could be reasonably located, although individual atoms were not all resolved. Two consecutive refinements reduced the reliability factor from 0·35 to 0·25 and thus confirmed the structure derived from the a-axis projection.

FIG. 4a.

FIG. 4b.

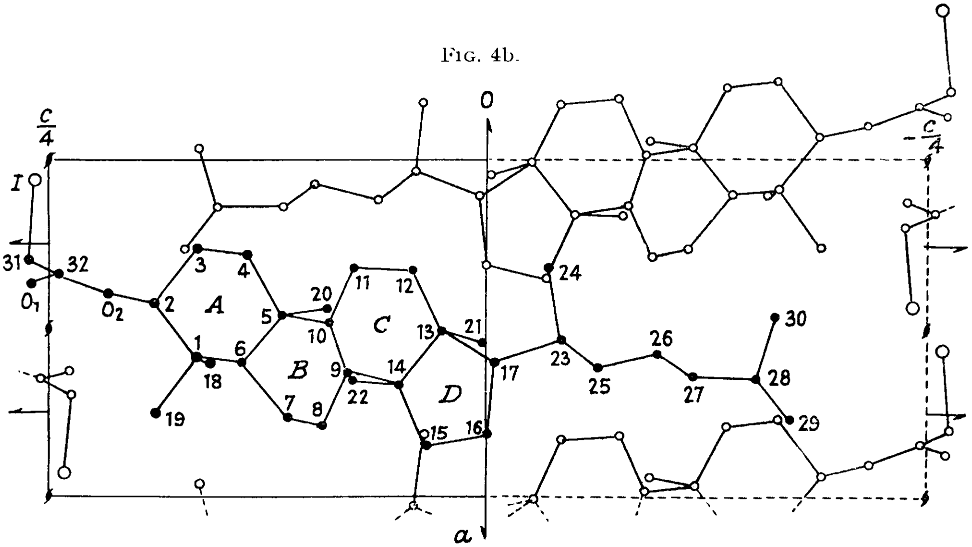

FIG. 4a. *The electron-density distribution projected on* (010).
FIG. 4b. *The corresponding diagram of the crystal structure. The molecule* (i.e. *the asymmetric unit*) *is shown in thick lines while parts of two related molecules appear in thinner lines.*

By making minor adjustments in atomic parameters indicated by a comparison of the two projections, the reliability factors were reduced finally to 0·21 and 0·22 for the $0kl$ and $h0l$ structure amplitudes respectively (Table 1). The final contour map of the a-axis projection is shown in Fig. 2, a similar projection extending over several unit cells in Fig. 3a with the corresponding molecular diagram in Fig. 3b. This shows the packing of molecules in the crystal. The contour map of electron density projected down the b axis is shown in Fig. 4a, with an interpretive diagram in Fig. 4b.

The parameters of all 35 atoms of the asymmetric unit (molecule) are listed in Table 2, the origin being the same as that given for space group $P2_12_12_1$ in " International Tables " (*loc. cit.*). The atoms $C_{(1)}$ to $C_{(30)}$ are numbered as for triterpenes [see (I) and Fig. 4b]. The intramolecular bond lengths calculated from these parameters are given in Table 3 with a selection of the smaller intermolecular approach distances.

DISCUSSION

The resolution of atoms obtained in this analysis is less than can be achieved for smaller molecules, mainly owing to the large temperature factor restricting the number of observed reflections. As a result, the bond lengths can be quoted only to within 0·09 Å, but are sufficiently precise to define adequately the structure and stereochemistry of lanostenyl iodoacetate and hence of lanostenol provided that there is no inversion. The approach distances between molecules correspond to van der Waals bonds.

The existence of the double bond in the molecules between $C_{(9)}$ and $C_{(10)}$ can be deduced from the two projections independently of any chemical evidence, thus the planarity of $C_{(5)}$, $C_{(8)}$, $C_{(9)}$, $C_{(10)}$, $C_{(11)}$, and $C_{(18)}$, associated with the double bond modifies the regular zig-zag which would be expected in a fully hydrogenated *trans*-fused ring system. This aspect is clearly shown in Figs. 3a and b. In the second projection, the angular disposition of the group $C_{(5)}$--$C_{(14)}$ associated with the double bond is revealed in Figs. 4a and b. If no strain were involved, this double bond would confer a symmetrical relationship on rings B and C in that $C_{(7)}$ would be symmetrically disposed with respect to $C_{(12)}$ and $C_{(6)}$ to $C_{(13)}$ across the centre of the double bond. However, it was noted in the *b*-axis projection particularly that $C_{(12)}$ was displaced from the expected position (compare the projected distances $C_{(7)}$–$C_{(8)}$ and $C_{(11)}$–$C_{(12)}$). Consideration of a simple ball-and-rod model showed that the observed displacement of $C_{(12)}$ was in agreement with the shift produced as a result of the fusion of the five-membered ring D to the six-membered ring C. The *trans*-fusion C–D involved considerable strain, which was partially relieved by the movement of $C_{(12)}$. Although a minor point, this was satisfactory confirmation of the correctness of the structure which had been deduced. The bonds $C_{(1)}$–$C_{(18)}$ and $C_{(5)}$–$C_{(20)}$ should lie parallel if ring A is regular, but there is considerable steric hindrance between the methyl groups which is relieved by a lateral displacement (see Fig. 3).

The evidence for the linkage of the side chain to the ring system at $C_{(17)}$ is as follows. When the analysis was being carried out, chemical evidence could not determine whether ring D was six- or five-membered. In the *a*-axis projection, it is clear that if ring D is six-membered, then the projected distance between [$C_{(16)}$, $C_{(17)}$] and $C_{(23)}$ should be approximately 0·90 Å., *i.e.*, similar in distribution to *RS* (Fig. 3), whereas the observed value *i.e.*, *PQ*, is at least 1·5 Å. This distance must correspond to a single carbon–carbon bond, lying almost parallel to (100). Hence ring D must be five-membered, the ring system terminating at *P*, and the two atoms at *Q* (indicated by the peak height in the contour map) must lie one above the other and must correspond to the first atom of the side chain with an associated methyl group. From this projection, it could be inferred that the side chain was attached to $C_{(16)}$ or $C_{(17)}$, but could not possibly be associated with $C_{(15)}$. Consideration of the *b*-axis projection revealed that the point of linkage is $C_{(17)}$ (cf. Fig. 4).

The structural formula deduced for lanostenol in the present study is given by (I). The arrangement of (I) has been brought into line with those of the steroids; this is contrary to the convention for triterpenoids, but the latter appears to have outlived its convenience and will cause confusion when the stereochemistry of the compounds is to be compared with that of the steroids for which a widely-used standardisation has been achieved (Fieser and Fieser, " Natural Products related to Phenanthrene," Reinhold, New York, 1949; *J.*, 1951, 3532). Halsall, Jones, and Meakins (*J.*, 1952, 2862) have made a similar modification. The numbering for triterpenoids has been preserved, however, to prevent confusion, but the stereochemistry of lanostenol has been based on the convention accepted for steroids (*loc. cit.*).

The molecule of lanostenol, like those of many steroids (Bernal, Crowfoot, and Fankuchen, *Trans. Roy. Soc.*, **1940**, *A*, **239**, 135), is flat and lath-shaped, of dimensions 20 × 6 × 5 Å.

Ring A (cf. Fig. 3) is of the " chair " or " Z " type, ring B is *trans*-fused to ring A, while rings B and C share the double bond $C_{(9)}$–$C_{(10)}$ which imposes planarity on the atoms $C_{(5)}$--$C_{(14)}$. The general disposition of the composite B–C ring system is of " chair " type with atoms $C_{(6)}$ and $C_{(7)}$ above and $C_{(12)}$ and $C_{(13)}$ below the plane $C_{(5)}$--$C_{(14)}$. This is shown in Fig. 3. Rings C–D are *trans*-fused. Because rings A–B are *trans*-fused, the relation of the $C_{(5)}$-methyl group is fixed and is considered as β-oriented (Fiesers' notation). The hydroxyl group is attached to $C_{(2)}$ and is β-oriented or equatorial (Barton, *Experientia*, 1950, **6**, 376). The $C_{(18)}$–$C_{(19)}$-*gem*-dimethyl group is adjacent to the hydroxyl group; this agrees with chemical evidence. The $C_{(13)}$- and $C_{(14)}$-methyl groups are β- and α-oriented, respectively, the bonds, $C_{(13)}$–$C_{(14)}$ and $C_{(14)}$–$C_{(22)}$, being non-parallel, owing to the distortion imposed by the *trans*-fusion of C–D. The side chain is β-oriented with respect to $C_{(17)}$. The disposition of the side chain is such as to bring $C_{(24)}$, $C_{(29)}$, and $C_{(30)}$ approximately coplanar with the ring system, leaving only the four methyl groups at $C_{(18)}$, $C_{(20)}$, $C_{(21)}$ and $C_{(22)}$ projecting from the general plane of the molecule.

The equatorial position of the ring-A hydroxyl group and the " chair " configuration of this ring are in accord with the generally accepted view (Barton, *loc. cit.*; Hassel, *Research*, 1950, **3**, 504) that these dispositions are more stable than the polar position of the bond or the movable " boat " formation of the ring. In addition, it appears that when two rings are fused through a double bond the composite ring system in a " chair " form is more stable than one of a boat formation. A model of the lanostenol molecule is shown in Fig. 4b.

The structural formula for lanostenol is in agreement with the partial formula proposed recently by Ruzicka *et al.* (*loc. cit.*) and Barton, McGhie, *et al.* (*loc. cit.*), based on chemical evidence and study of the infra-red and ultra-violet spectra of derivatives. The *X*-ray analysis has however determined unambiguously the point of linkage of the side chain to the ring system and has provided a complete description of the stereochemistry, independently of chemical evidence.

Lanostadienol (II) differs from lanostenol only in the existence of a $C_{(27)}$–$C_{(28)}$ reactive double bond and can therefore be assumed to have the same configuration as lanostenol with only a minor steric modification of the side chain. All chemical evidence points to agnostadienol (III) and agnostatrienol (IV) having the same structural skeleton, which will therefore be similar to that of lanostenol, apart from steric modifications due to the presence of the two inert double bonds and the consequent planarity of the adjacent atoms.

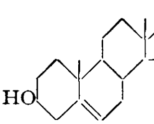

(V)

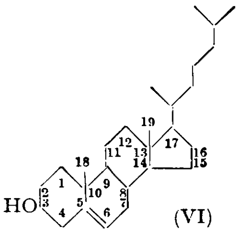

(VI)

The skeleton of the wool-wax triterpenes bears a close resemblance to the steroid nucleus (V) (except for the position of the double bond) while the position of the hydroxyl group and of $C_{(5)}$ (steroid $C_{(10)}$) and of $C_{(13)}$ (steroid $C_{(13)}$)-methyl groups are the same. In addition, the side chain is attached to $C_{(17)}$ in both steroids and triterpenoids. Comparison of Fig. 4b with Carlisle and Crowfoot's model of cholesterol (VI) (*loc. cit.*, Fig. 10) reveals a striking similarity. Lanostenol differs structurally from cholesterol only in the position of the double bond and in the addition of the three methyl groups, at $C_{(18)}$, $C_{(19)}$, and $C_{(22)}$. There was, however, no similarity in the crystalline forms, cholesteryl iodide being monoclinic and lanostenyl iodoacetate orthorhombic.

The authors thank Mr. R. G. Curtis of the Organic Chemistry Section for many helpful discussions regarding the chemistry of lanostenol.

CHEMICAL PHYSICS SECTION, DIVISION OF INDUSTRIAL CHEMISTRY,
C.S.I.R.O., MELBOURNE, AUSTRALIA.
[*Received, December 29th*, 1952.]